Incorporating pedotransfer functions into the MOSEE model to simulate runoff and soil erosion at different scales

EDUARDO E. DE FIGUEIREDO[1] & ANTHONY J. PARSONS[2]

1 *Department of Civil Engineering, Federal University of Campina Grande/Brazil, PO Box 505, Campina Grande/PB, Brazil*
eduardo@dec.ufcg.edu.br

2 *Department of Geography, University of Sheffield, Winter Street, Sheffield S10 2TN, UK*

Abstract The distributed MOSEE model was used to investigate scale and land-use change impacts on runoff and soil erosion processes in catchments located in the semi-arid northeast region of Brazil. The model includes functions that take into account the spatial variability of rainfall and catchment characteristics. To simulate hydrological and sediment transport processes in the study basins, model parameters were estimated with previously published pedotransfer functions and soil texture data in the Representative Sumé basin (RBS) located in Paraiba, Brazil. The results show that, in general, runoff and sediment yield simulations were comparable to the observed values at the small scale using a combination of pedotransfer functions. For the larger basins, the simulated runoffs, aggregated to a daily basis for comparisons, provided a reasonable fit for the observed data in two catchments. The simulated runoff and sediment yields increased as deforestation and catchment area increased, demonstrating the relevance of vegetation as an effective protective agent to reduce soil erosion.

Key words physically-based model; parameterization; pedotransfer function; simulation; distributed model MOSEE

INTRODUCTION

Distributed physically-based models require parameters not generally measured in the field (i.e. flow dynamics in the unsaturated zone); however, these parameters can be estimated using pedotransfer functions previously published in the literature. The role of such functions is to characterize the soil matrix potential, hydraulic conductivity, soil moisture content, soil tension and soil moisture content relationships. Pedotransfer functions are available for a range of soils worldwide (e.g. Wagner *et al.*, 2001), but they have not been widely used in simulation models and tested extensively with data observed in the field. In this paper, pedotransfer functions were used in the soil erosion model MOSEE (Figueiredo *et al.*, 2009) to simulate runoff and soil erosion processes in small and large catchments in Paraíba, Brazil. The paper investigates the utility of the model to simulate and examine scale effects and land-use change impacts on runoff and soil erosion processes. The paper reports the model development and modelling results.

THE MOSEE MODEL

The MOSEE model includes functions that account for catchment variability in hydrological processes. The basin system is subdivided into sub-catchments linked to the river and includes a representation of three soils layers where the vertical and horizontal fluxes occur in the soil. Rainfall intensity (i) is space-variant and based on input data from meteorological stations. Interception is represented by the interception depth (I_t), which reflects the average depth of rainfall retained by any particular vegetation type, and the volume of interception depends on the proportion of area covered by grass and rocks (C_r) and canopy (C_g) (Figueiredo, 2009).

Actual evapotranspiration rates (E_a) are set to zero during rainfall and/or when the soil tension ψ is <1500 kPa (wilting point). The Penman equation modified by Monteith (1965) is used to determine E_a, which assumes the potential value (E_p) when ψ_{fc} < 33.3 kPa (field capacity). Between rainfall events, E_a is determined according to a nonlinear relationship between the ratio of actual to potential evapotranspiration and soil tension, $E_a/E_p = \kappa.f(\psi)$, where κ is a soil factor (Feddes & Zaradny, 1978). The potential evapotranspiration (E_p) can be determined using pan-data or alternative methods described by Chow *et al.* (1988) and Shaw (1994). Soil tension is

Copyright © 2010 IAHS Press

determined using the equation $\psi = A\theta^B$, where A and B are soil parameters depending on clay and sand percentages (%C and %S), and θ is the volumetric soil moisture content (Saxton *et al*., 1986). Since this equation is valid for 10 kPa < ψ < 1500 kPa, it is assumed that if $\psi \leq 10$ kPa then $\theta = \theta_s$ (the saturated soil moisture content), with θ_s taken as porosity (ϕ) corrected by f_{air}, a factor for the air entrapment ($0.8 < f_{air} < 0.9$), that is $\theta_s = f_{air}\phi$. Soil porosity can be input to the model as an observed value (and also θ_s), or alternatively determined using the bulk density of the soil and of quartz (2.65 g/cm^3). Surface infiltration capacity (f) is determined using the volumetric soil moisture content (θ) with a potential function, $f = C_t\,(\theta)^{D_t}$, or a function of the Horton type, $f = f_c + (f_o - f_c)e^{k\theta}$, whose parameters C_t and D_t (potential), f_o, f_c and k (Horton) can be calibrated or quantified directly in field experiments. The averaged infiltrated lamina over the time interval Δt corresponds to the product $i.\Delta t$ if $i < f$, or to the product $\Delta t\,(f_t + f_{t-\Delta t})/2$ if $i > f$, which vary with the surface slope. The infiltrated lamina will percolate through the soils layers and affect the soil moisture content profile.

Percolation in the unsaturated zone is determined according to the lowest hydraulic conductivity of two adjacent layers, and will occur if the soil moisture content of the upper layer is greater than the value corresponding to the soil tension of 10 kPa (for $\psi > 10$ kPa the soil moisture content decreases rapidly, and as a consequence, the soil hydraulic conductivity). If the hydraulic conductivity of the upper layer (K_A) is greater or equal to the hydraulic conductivity of the middle layer (K_B), then percolation occurs at the rate of K_B. Otherwise, percolation is at the rate of K_A. The same applies to the lower layer. In the model, if $K_B \geq K_C$ then water will percolate from layer B to layer C at the rate of K_C, or otherwise, at the rate of K_B.

The non-saturated hydraulic conductivity of the soils (K_A, K_B, K_C) can be determined with one of the following methods: Brooks & Corey (1964), Campbell (1974), Saxton *et al.* (1986), or Van Genuchten (1980), which all depend on the relative saturation (except the equations of Campbell, 1974, and Saxton *et al*., 1986), $S_e = (\theta - \theta_r)/(\theta_s - \theta_r)$, where θ_r is the residual moisture content determined with the equation of Rawls & Brakensiek (1989), and on the saturated hydraulic conductivity (K_s) determined, alternatively, with the equations of Saxton *et al.* (1986), Rawls *et al.* (1998), Brakensiek *et al.* (1984), or Cosby *et al.* (1984), all of them are based on %C and %S. The equation of Rawls *et al.* (1998) for the saturated hydraulic conductivity also depends on the field capacity moisture content (θ_{fc}) determined with the Saxton *et al.* (1986) equation. In general all the pedotransfer functions used are valid for %S ≥ 5% and 5% ≤ %C ≤ 60%.

The volumetric soil moisture content is determined in the model for two conditions: (a) between rainfall events, and (b) during rainfall events. Between rainfall events, the variations of soil moisture content of the surface layer A are determined based on the mass conservation equation, and on the Darcy equation for vertical flow, which is combined and expressed in terms of finite difference to produce the following equation:

$$\theta_{A(t+\Delta t)} - \theta_{A(t)} = -\frac{\Delta t}{h_A}\left[\frac{K_A(\theta)\psi_A(\theta)}{h_A}\right] - \frac{\Delta t}{h_A}K_A(\theta) - \frac{\Delta t}{h_A}E_a[\psi(\theta)] \qquad (1)$$

Equation (1) is applied under conditions of non-hysteresis and is used in the model to determine the surface layer soil moisture content variations over time. By attributing a value for the moisture content at the initial time $\theta_{A(t)}$, the non-saturated hydraulic conductivity, soil tension and actual evapotranspiration can be determined with the equations previously mentioned, as well as the actual moisture content of the surface layer $\theta_{A(t+\Delta t)}$. The initial soil moisture content value of each soil layer can be input to the model as directly measured values or calculated as a proportion of soil porosity. Conversely, it can also be used as the moisture content corresponding to wilting point determined with the equation of Saxton *et al.* (1986), that is $\theta_t = \theta_{wp} = (1500/A)^{1/B}$. The moisture content of the sub-surface layer B, θ_B, will decrease by evaporation if $\theta_A \leq \theta_{10}$ (the minimum value up to which the water cannot percolate to the sub-surface layer that corresponds to 10 kPa, determined with the equation of Saxton *et al.* (1986), i.e. $\theta_{10} = (10/A)^{1/B}$). Otherwise the soil moisture content θ_B will increase based on the lowest hydraulic conductivity of the adjacent layers. The same condition applies for the third layer. The moisture content variations for these

conditions are: $\Delta\theta_B = K_m.\Delta t/h_B$ if $\theta_A > \theta_{Amin}$ or $-E_a.\Delta t/h_B$ if $\theta_A \leq \theta_{Amin}$, and $\Delta\theta_C = K_m.\Delta t/h_C$ if $\theta_B > \theta_{Bmin}$ or $-E_a.\Delta t/h_C$ if $\theta_B \leq \theta_{Bmin}$, where K_m is the lowest hydraulic conductivity of the two adjacent layers, i.e. $K_m = K_B$ if $K_B < K_A$ or $K_m = K_A$ otherwise (layer B), and $K_m = K_C$ if $K_C < K_B$ or $K_m = K_B$ otherwise (layer C), with K_A, K_B and K_C representing average values over the time interval Δt.

When rainfall occurs, $E_a = 0$ and, therefore, the moisture content of the surface layer increases according to the infiltration capacity if $i > f$, or according to the rainfall intensity. For the sub-surface layer (B) and the layer underneath (C), the approach is similar to the case when rainfall does not occur. These conditions are: $\Delta\theta_A = f.\Delta t/h_A$ if $i > f$ or $\Delta\theta_A = i.\Delta t/h_A$ if $i \leq f$ (layer A), $\Delta\theta_B = K_A.\Delta t/h_B$ if $K_A < K_B$ or $\Delta\theta_B = K_B.\Delta t/h_B$ if $K_A \geq K_B$, and $\Delta\theta_C = K_B.\Delta t/h_C$ if $K_B < K_C$ or $\Delta\theta_C = K_C.\Delta t/h_C$ if $K_B \geq K_C$, with the infiltration capacity f and hydraulic conductivities being averaged value over the time interval Δt.

The sub-surface flow is determined with equation (2), which is based on the Darcy equation, assuming: (a) isotropic and non-confined conditions; (b) the interflow discharges at the soil surface with zero hydraulic head, when the soil surface moisture content is greater or equal to the value corresponding to field capacity; (c) the interflow does not change markedly over short time intervals; (d) the mean hydraulic head is $h = h(\theta)$. These conditions combined produce the following equation, where $K(\theta > \theta_{fc})$ is the hydraulic conductivity, L is the extension of the sub-surface flow along the catchment of area A_b.

$$I_{sb} = \frac{K(\theta)[h(\theta)]^2}{3600}\frac{L^2}{A_b} \quad \text{if } \theta > \theta_{\text{fc}} \tag{2}$$

The model considers groundwater flow and the interaction between the river and bank soil. Water from the river will discharge into the bank soil if the channel water level (h_c) is above the water table level (h_{wt}). Otherwise, the groundwater will discharge into the river. In both cases, equation (2) is used to determine the discharge by replacing I_{sb} with I_{gw}, $K(\theta)$ with $K(\theta_s)$, and $h(\theta)$ *with* $h_c^2 - h_{wt}^2$ if $h_c > h_{wt}$, or for $h_{wt}^2 - h_c^2$ if $h_{wt} > h_c$. No interaction between the channel and bank soil will occur if the water table level is below the channel bed but groundwater flow (I_{gwi}) can be input to the model.

Overland flow, calculated as the sum of the surface, sub-surface and groundwater flows, can be routed to downstream reaches using the convex procedure of the SCS/USA (McCuen, 1982) or the method of Muskingum (Chow *et al.*, 1988), with the wave translation time determined with the method of Kirpich (1940) or with the method of Kerby (1959).

The sediment component includes the soil erosion by raindrop impacts and by runoff. Erosion by rainfall is based on the squared moment for rainfall, and by runoff on the Shields' critical shear stress, which can be adjusted by the rainfall and runoff erosivity coefficients (k_r and k_f). Sediment detached by rainfall (E_r) and runoff (E_f) are combined to simulate the total sediment load ($E = E_r + E_f$) provided for transport that depends on the sediment transport capacity of a given flow (T_c). If $E > T_C$ the difference represents deposition (feedback is not considered). The flow transport capacity is modelled alternatively with the equations of Engelund & Hansen (1967), Yalin (1963) or Laursen (1958) that take into consideration the sediment size distribution of the eroded soil. The effect of flow depth and ground cover in reducing raindrop impact are accounted for in the model.

RUNOFF AND SOIL EROSION MODELLING

Runoff and soil erosion modelling were investigated through simulations carried out for one bare cleared micro-basin (5200 m^2), and for the three vegetated basins of the RBS (Fig. 1): Umburana (10.7 km^2), Jatobá (26.8 km^2) and Gangorra (137.4 km^2), where there is a medium relief with altitudes varying from 780 m in the west to 540 m in the east, and a bush type of vegetation namely Caatinga (Cadier & Freitas, 1982). All study catchments were divided into 20 sub-basins. The micro-basin was modelled globally and divided into 4 sub-basins for sensitivity analysis. The model parameters were all set based on the characteristics of the RBS soil that is shallow in about

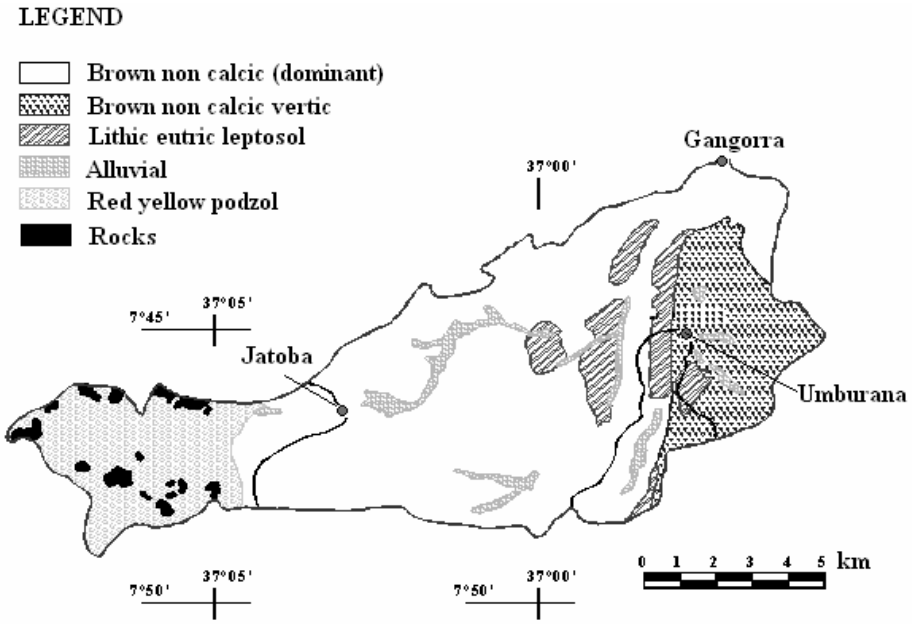

Fig. 1 Soils of the Sumé basin (RBS).

80% of the area (10–50 cm), consisting of two main soil types: a loam top soil (15.77 %C and 50.2 %S; 10-cm thick) and a clay loam soil underneath (32.5 %C and 50.2 %S; 40-cm thick). Within the sub-basin of Jatobá, the soil is deeper (100–200 cm) and more permeable than the other soils in the RBS. For the micro-basin simulations breakpoint precipitation, hydrographs and sediment load data collected in 1986 were used, while for the simulations in the basins of the RBS breakpoint data of rainfall, collected in 1977, and daily hydrographs (soil erosion was not observed in the RBS) were utilized. These sites were studied for 10 years (1982–1990) and provided a relevant pool of data for analyses and modelling (see details in Figueiredo, 1998; Cadier & Freitas, 1982).

The Jatobá and Umburana sub-catchments were divided into equal areas of contribution, reaches and elevations, while the RBS division varied according to the relief (the upper part in 4 divisions, the middle in 12, and the lower part in 4 sub-basins). Parameters and methods used to parameterize the model are: the method of Kirpich, 1940 (time of concentration), the propagation convex method of the SCS/USA (McCuen, 1982) with time steps less than 1 minute (micro-basin), and between 10 and 23 minutes (other basins), the moisture content at saturation $= f_{air}.\phi$, with porosity estimated with the equation of Saxton *et al* (1986), and $f_{air} = 0.91$ (layer A), and $f_{air} = 0.8$ (layers *B* and *C*), the initial moisture content $= \theta_{wp}$ estimated with the equation of Saxton *et al.* (1986), the surface infiltration capacity $f = C_t(\theta)^{D_t}$ with $C_t = 7.0$ and $D_t = -0.8$ (micro-basin and Umburana) and $C_t = 2.5$ and $D_t = -1.5$ (Gangorra and Jatobá), the equation of Saxton *et al.* (1986) for the saturated hydraulic conductivity (micro-basin), and Cosby (1984) for the other catchments, the equation of Brooks & Corey (1965) for the non-saturated hydraulic conductivity with its exponent modified $\eta = -1/\lambda$ with $\lambda = -B$ of Saxton *et al.* (1986), observed potential pan-evaporation (E_p) data, $Ea/Ep = \kappa.f(\psi)$ with $\kappa = 10$, Manning roughness coefficient equal to 0.02 (micro-basin), and equal to 0.03 (other basins), channels width of 0.5 m (micro-basins), 10 m (Jatobá and Umburana) and 10–30 m (Gangorra), channel slope of 0.07 m/m (micro-basin), 0.045 m/m (Jatobá and Umburana) and 0.04–0.07 m/m (Gangorra), $C_g = C_r = 0$ for the micro-basin (bare cleared), 0.05 (Jatobá and Umburana) and 0.05–0.15 (Gangorra), interception depth $I_t = 0$ (micro-basin) and 0.5 mm (other basins), the erosivity coefficients $k_r = 7.5$ s^2 kg^{-1} m^{-2} and $k_f = 0.0003$ kg.m^{-2}s^{-1}, the Engelung & Hansen equation for the transport capacity by the flow. The representative sediment diameter $D_{50} = 0.4$ mm (micro-basin), which was obtained from sieve analysis of the eroded soils at the study site, and 0.5 mm (other basins). Vegetation parameters I_t, C_g and C_r for the RBS basins were changed to zero for analysis of land-use change impact on runoff.

RESULTS AND DISCUSSION

Figures 2–6 provide examples of model simulations for all the catchments of the RBS. Table 1 shows simulated annual values for vegetated and non-vegetated conditions of the catchments to analyse annual runoff and soil erosion at the investigated scales under different surface cover conditions.

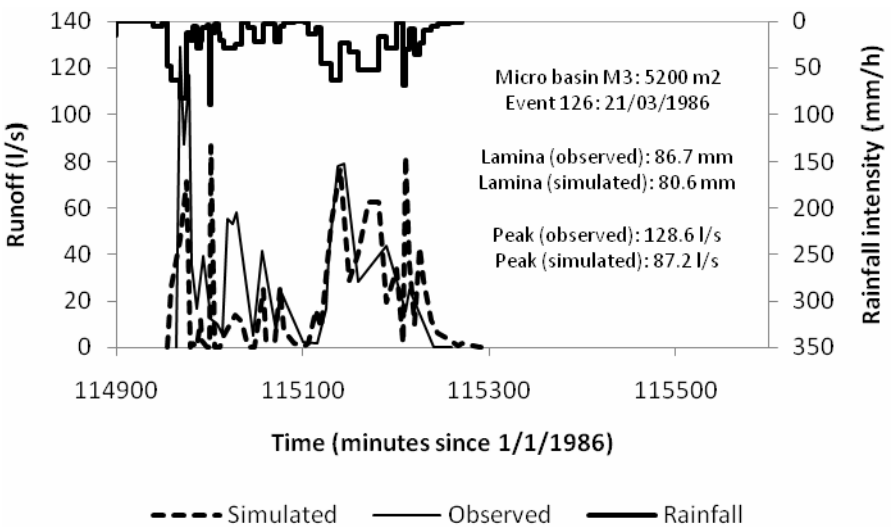

Fig. 2 Simulated and observed hydrographs (Event 126 – Micro-basin: 20 sub-basins).

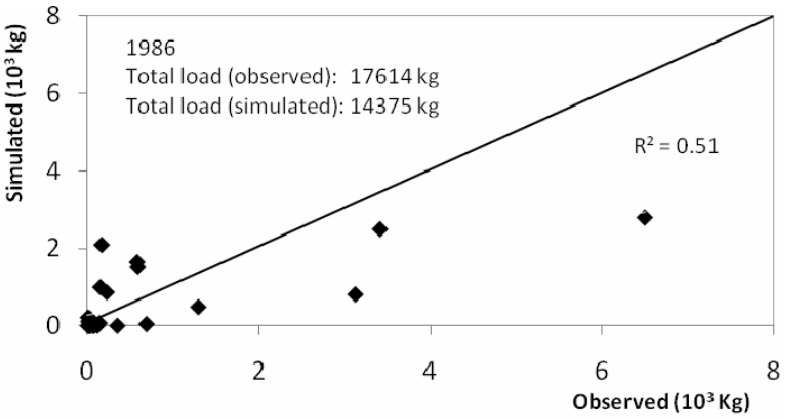

Fig. 3 Simulated and observed sediment loads in 1986 (Micro-basin: 4 sub-basins).

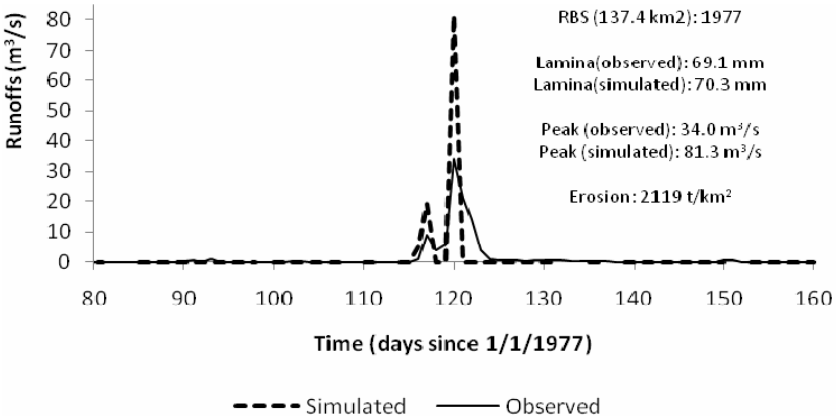

Fig. 4 Simulated and observed daily hydrographs at Gangorra.

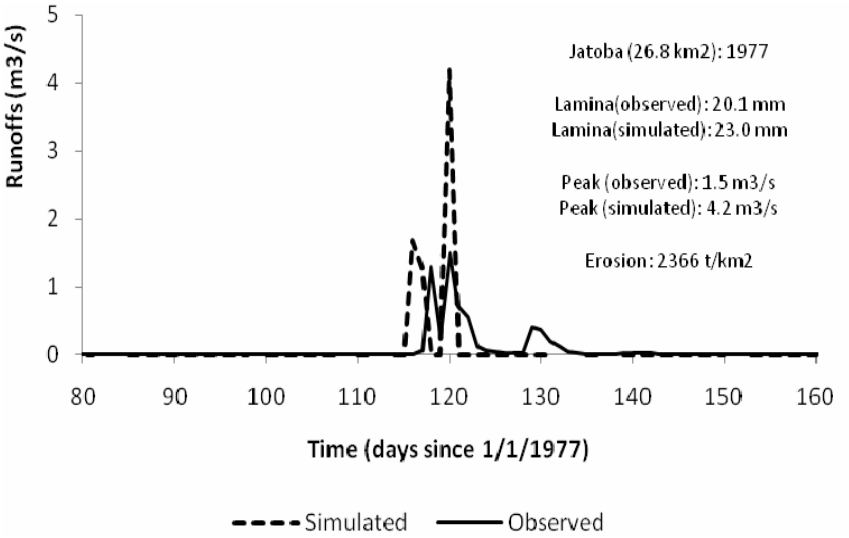

Fig. 5 Simulated and observed daily hydrographs at Jatobá.

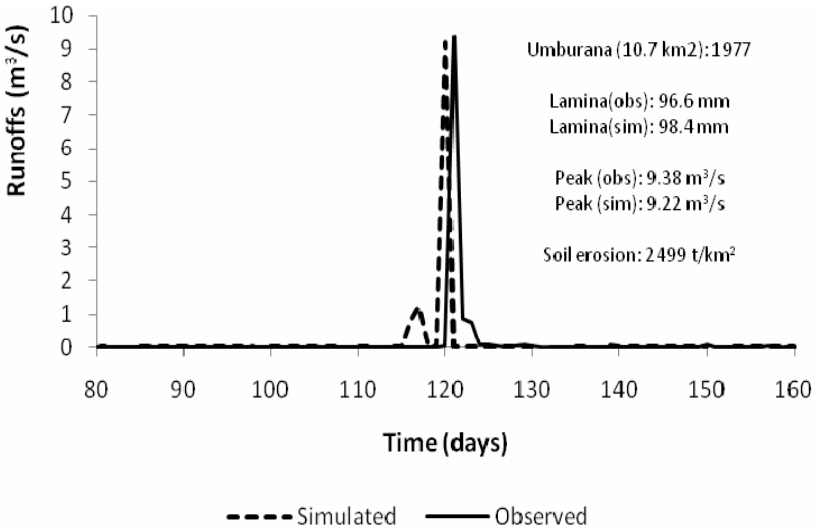

Fig. 6 Simulated and observed daily hydrographs at Umburana.

Table 1 Annual results for vegetated (VG) and non-vegetated (NVG) conditions of the catchments.

Catchment	Vegetation Condition	Year	Laminas (mm) Obs	Laminas (mm) Sim	Peaks (m^3/s) Obs	Peaks (m^3/s) Sim	Sediment (t) Obs	Sediment (t) Sim
M3 (0.0052 km^2)	VG	1986	270	240	0.129	0.193	17.6	13
	NVG			276		0.210		21
Umburana (10.7 km^2)	VG	1977	97	98	9.4	9.2		26742
	NVG			101		9.4		29884
Jatoba (26.8 km^2)	VG	1977	20	23	1.5	4.2		63421
	NVG			24		4.4		69932
Gangorra (137.4 km^2)	VG	1977	69	70	34	81		291220
	NVG			87		97		429303

In general, the model results were somewhat consistent with the observed data at the micro-basin scale. Coefficients of determination (R^2) for hydrographs, laminas and sediment yields were

0.8 (hydrology) and 0.49 (sediment). The results for the divisions of the micro-basin were quite similar (~240 mm for the 4 and 20 divisions of the scale), but slightly overestimated (380 mm) the observed (270 mm) annual runoff when simulated globally. In addition, the simulated sediment loads ranged from 13 to 18 t, compared to the measured value of 21 t. For the larger catchments of the RBS, the observed daily hydrographs were poorly simulated for the Jatobá catchment (R^2 > 0.35) but better represented for the Gangorra catchment (R^2 > 0.63). At Umburana, the simulated peak discharge (9.22 m^3/s) was close to the observed one (9.38 m^3/s) but the hydrograph was poorly represented over time. Although the values of R^2 were not generally good, the pedotransfer functions based on soil texture used to parameterize the model produced reasonable results given that the soil–water parameters were not calibrated. The model did not produce significant sub-surface flow, which is consistent with observations in the study region where runoff is predominantly generated by excess of rainfall intensity over infiltration capacity, or by saturation of the surface layer during periods of continuous and intense rainfall. Investigations on the effect of a water table placed at the level of 50 cm above the channel bed and a value of I_{gwi} varying from 1 to 1000 L/s on discharge showed no significant contribution for values of I_{gwi} from 1 to 100 L/s, but increased 2-fold for I_{gwi} = 500 L/s and 3-fold for I_{gwi} = 1000 L/s. The soil erosion did not increase markedly (291 220 to 295 479 t) as I_{gwi} increased from 1 to 1000 L/s. The simulations were affected by scale and land use, increasing as basin area and deforestation increased.

CONCLUSIONS

The results of this study show that: (a) the MOSEE model was adequately parameterized with previously published pedotransfer functions and the model provided comparable simulations of measured runoff and soil erosion in small and large catchments in the semi-arid Cariri region in the Paraíba state of Brazil; (b) runoff was less sensitive to deforestation than soil erosion; and (c) runoff and soil erosion simulations increased consistently with increasing scale.

Acknowledgements CAPES/Brazil (Coordenação de Aperfeiçoamento de Pessoal de Nível Superior) is acknowledged for the post-doctoral scholarship awarded to the first author, CNPQ/Brazil (Conselho Nacional de Desenvolvimento Científico e Tecnológico) for supporting the Project MODHIPB (Grant no. 474430/2006-5), the Academic Unit of Civil Engineering, Federal University of Campina Grande (UFCG), Paraíba, Brazil, in allowing the first author to conduct this research, the Department of Geography, University of Sheffield, UK, for receiving the first author as a Research Associate, and Professor Anthony Parsons, from the Department of Geography, University of Sheffield, UK, for his acceptance in supervising the post-doctoral research.

REFERENCES

Blaney, H. F. & Criddle, W. D. (1950) Determining water requirements in irrigated area from climatological irrigation data. US Department of Agriculture, Soil Conservation Service, Tech. Pap. no. 96, 48 pp.

Brakensiek, D. L., Rawls, W. J. & Stephenson, G. R. (1984) Modifying scs hydrologic soil groups and curve numbers for rangeland soils. ASAE Paper no. PNR-84-203, St. Joseph, Michigan, USA.

Brooks, R. H. & Corey, A. T. (1964) Hydraulic properties of porous media. Hydrol. Paper no. 3, Colorado State Univ., Fort Collins, USA.

Cadier, E. & Freitas, B. J. (1982) Bacia representativa de Sumé. Primeira estimativa de água. Série Hidrologia no. 14, SUDENE, Recife, Pe, Brazil (in Portuguese).

Campbel , G. S. (1974) A simple model for determining unsaturated conductivity from moisture retention data. *Soil Sci.* **117**, 311–314.

Chow, V. T., Maidment, D. R. & Mays, L. W. (1988) *Applied Hydrology*. McGraw-Hill Int. Ed., New York, USA.

Cosby , B. J., Hornberger, G. M., Clapp, R.B. & Ginn, T. R (1984) A statistical exploration of the relationship of soil moisture characteristics to the physical properties of soils. *Water Resour. Res.* **20**(6), 682–690.

Engelund, F. & Hansen, E. (1967) *A Monograph on Sediment Transport in Alluvial Streams*. Teknisk Vorlag, Copenhagen, Denmark.

Feddes, R. A. & Zaradny, H. (1978) Numerical model for transient water flow in non-homogeneous soil-root systems with groundwater influence. In: *Modeling, Identification and Control in Environmental Systems* (ed. by Vansteenkieste, G.C). IFIP North-Holland Publishing Company, The Netherlands.

Figueiredo, E. F. (1998) Scale effects and land use change impacts in sediment yield modelling in a semi-arid region of Brazil. PhD Thesis. The University of Newcastle upon Tyne, UK.

Figueiredo, E. F. (2009) MOSEE, a model for soil erosion estimation. Documentation. Post doctoral project carried out in the University of Sheffield/UK. Supported by CAPES/BRAZIL Oct. 2008–Sep. 2009.

Kerby, W. S. (1959) Time of concentration for overland flow. *ASCE Civil Engineering* **29**(3).

Kirpich, Z. P. (1940) Time of concentration of small agricultural watershed. *ASCE Civil Engineering* **10**(6).

Laursen, E. M. (1958) The total sediment load of streams. *J. Hydraul. Div. ASCE* **54**, 1–36.

McCuen, R. H. (1982) *A Guide to Hydrologic Analysis Using SCS Methods*. Prentice-Hall, Inc., Englewood Cliffs, New Jersey, USA.

Monteith, J. L. (1965) Evaporation and environment. In: *The State and Movement of Water in Living Organisms* (Proc. 15th Symposium for Experimental Biology, Swansea), 205–234. Cambridge University Press, London, UK.

Penman, H. L. (1948) Natural evaporation from open water, bare soil and grass. *Proc. Roy. Soc. London* **A193**, 120–145.

Rawls, W. J. & Brakensiek, D. L. (1989) Estimation of soil water retention and hydraulic properties. In: *Unsaturated Flow in Hydrologic Modeling – Theory and Practice* (ed. by H. J. Morel-Seytoux), 275–300. Kluwer Academic Publisher, Dordrecht, The Netherlands.

Rawls, W. J., Gimenez, D. & Grossman, R. (1998) Use of soil texture, bulk density and slope of the water retention curve to predict saturated hydraulic conductivity. *Trans. ASAE* **41**(4), 983–988.

Saxton, K. E., Rawls, W. J., Rosemberger, J. S. & Papendick, R. I. (1986) Estimating generalized soil-water characteristics from texture. *Soil Sci. Soc. Am. J.* **50**, 1031–1036.

Shaw, E. M. (1994) *Hydrology in Practice*. Chapman and Hall. London, UK.

Van Genuchten, M. Th. (1980) A closed-form equation for predicting the hydraulic conductivity of unsaturated soils. *Soil Sci. Soc. Am. J.* **44**, 982–898.

Yalin, M. S. (1963) An expression for bed-load transportation. *J. Hyraul. Div. ASCE* **89**(HY3), 221–250.

Wagner, B., Tarnawski, V. R., Hennings, V., Müller, U., Wessolek, G. & Plagge, R. (2001) Evaluation of pedo-transfer functions for unsaturated soil hydraulic conductivity using an independent data set. *Geoderma* **102**, 275–297.

Yalin, M. S. (1963) An expression for bedload transportation. *J. Hydraul. Div. Proc. ASCE* **89**(HY3), 221–250.